

Experimental and Numerical Study of CO₂ Corrosion in Carbon Steel

Dr. Rana A. Majed

Materials Engineering Department, University of Technology /Baghdad
Email: Dr.rana_afif@yahoo.com

Dr. Ali H. Jawad

Materials Engineering Department, University of Technology /Baghdad

Dalia M. Jomaa

Materials Engineering Department, University of Technology /Baghdad

Received on: 3/10/2012 & Accepted on: 9/5/2013

ABSTRACT

This research involves study corrosion of low carbon steel under static and flow conditions at 200L/h in the absence and presence of CO₂ at two rates 9 and 30 ml/min at four temperatures by electrochemical method using potentiostat. Numerical model was achieved to compare between the experimental and theoretical results to estimate corrosion rate. The results show that the presence of CO₂ under static conditions shifts the E_{corr} toward noble direction, while under flow condition the presence of CO₂ shift E_{corr} toward active or noble direction at two rates of gas. The data of corrosion rate in mm/y indicate that the presence of CO₂ with two flow rate increased the rate compared with the case of absence of CO₂ under static conditions except one case, while under flow conditions, the presence of 9 ml/min. CO₂ increases the corrosion rate, while the presence of 30 ml/min. CO₂ decreases the rate because of formation FeCO₃ scale except at 298K. A Mathematical model was done which show the volumetric flow rate of CO₂ and finally the corrosion rate of CO₂ correlated with dimensionless groups and independent parameters.

Keywords: CO₂ Corrosion, Carbon Steel, Mathematical Model and Empirical Correlation.

دراسة نظرية وعملية لتآكل الستيل الكربوني بفعل غاز ثاني اوكسيد الكربون

الخلاصة

يتضمن هذا البحث دراسة تآكل الفولاذ واطيء الكربون ضمن الظروف الساكنة وظروف الجريان عند معدل سرعة ٢٠٠ لتر/ساعة بغياب وجود غاز ثاني اوكسيد الكربون عند معدلين من سرعة تدفق الغاز هي ٩ و ٣٠ مل/دقيقة وعند اربع درجات حرارية مختلفة بالطرق الكهروكيميائية باستخدام جهاز المجهاد الساكن. اجريت بعض الحسابات الرياضية للتنبأ بموديل رياضي لمقارنة النتائج النظرية مع العملية وتقدير معدل التآكل. اظهرت النتائج بان وجود غاز ثاني اوكسيد الكربون يزيح قيم جهد التآكل بالاتجاه الاكثر نبلاً ضمن الظروف الساكنة ولكلا معدلي تدفق الغاز. كما بينت نتائج معدل سرعة التآكل بوحدة المللي متر لكل سنة بان وجود الغاز يزيد التآكل مقارنة بحالة غياب الغاز في الوسط عند الظروف الساكنة ماعدا لحالة واحدة، بينما ضمن ظروف الجريان لوحظ بان وجود الغاز بمعدل سرعة التدفق ٩ مل/دقيقة يزيد معدل التآكل بينما وجود الغاز بمعدل تدفق مساوياً لـ ٣٠ يقلل معدل السرعة المعزى ربما الى تكون طبقة من كاربونات الحديدوز ماعدا عند درجة ٢٩٨ كلفن. بين الموديل الرياضي المنجز بان معدل التآكل المترابط مع المجاميع البعدية والمتغيرات غير المعتمدة في الجزء العملي.

INTRODUCTION

A variety of prediction models for CO₂ corrosion of carbon steel exist [1-15]. Most of these models are semi-empirical, or even fully empirical with only a handful of the more recent models being based on mechanistic descriptions of the processes underlying CO₂ corrosion [10-15]. Models for CO₂ corrosion have been developed by several investigators [16] in form of semi-empirical correlations, except system or electrochemical models for surface reactions. A particular challenge for model development has been the effect of iron carbonate scales [17].

There are many studies about CO₂ corrosion under static and flow conditions. Ethirajulu Dayalan et al. [18] studied characterization of the CO₂ corrosion prediction in pipe flow under FeCO₃ scale-forming conditions and they observed that the severity of corrosion depends on temperature, fluid characteristics (CO₂, partial pressure, gas/liquid ratio, water composition, water-to-oil ratio, pH), flow characteristics, and material characteristics; and under suitable conditions, corrosion products can form scales (FeCO₃) on the corroding surface. Anthony and Srdjan [19] studied prediction of two-phase erosion – corrosion in bends from the solution of the turbulent transport of species equation, the wall mass transfer coefficient can be calculated using the method of Nescic. Assuming mass transfer controlled corrosion, the mass transfer coefficient can be converted to local corrosion rate. Killian [20] studied jet impingement testing for flow accelerated corrosion. He described the basis of the disturbed flow correlation, and a procedure to relate the results of jet

impingement corrosion tests directly to corrosion in an operating system.

Energy Resour Technol [21] studied mass transfer coefficient measurement in water/oil/gas multiphase flow which provides fundamental knowledge towards the understanding of hydrodynamics and the subsequent effect on corrosion in pipelines. Rolf [22] studied corrosion control in oil and gas pipelines. Two of the most commonly used corrosion prediction models were combined with an oil and gas three phase fluid-flow model in order to be able to calculate corrosion rate profiles along a pipeline. Srdjan et al. [23] studied integrated CO₂ corrosion-multiphase flow model. Most of these models are semi-empirical, or even fully empirical with only a handful of the more recent models being based on mechanistic descriptions of the processes underlying CO₂ corrosion.

Shunsuke et al. [24] studied effects of water chemistry on flow accelerated corrosion and liquid droplet impingement accelerated corrosion. Overlapping effects of flow dynamics and corrosion are important issues in determining the reliability and lifetime of major structures and components in light water reactor plants.

Mohammed et al. [25] studied corrosion of carbon steel in high CO₂ environment, where in this study; flow-sensitive CO₂ corrosion has been investigated using a high-pressure high temperature rotating cylinder electrode (RCE) autoclave and a pipe flow loop system. Corrosion rates are measured via weight loss and by electrochemical methods at various pH's (3 to 5), temperatures (25 to 50°C), near critical and supercritical CO₂ partial pressures and at equivalent fluid velocities from 0 to 1.5 m/s. Asmara and Ismail [26] studied combinations effects of acetic acid in H₂S/CO₂ corrosion. This research proposed a prediction model incorporated with H₂S and CH₃COOH in CO₂ environments using a set of experiments. The experiments were conducted in the 3% NaCl solution saturated with 300 ppm of H₂S in CO₂ gas. Linear polarization resistance and electrochemical impedance spectroscopy methodology were used to study corrosion mechanism and to calculate carbon steel corrosion rate.

The aim of current work is to study effect of CO₂ corrosion at rates 9 and 30 ml/min for low carbon steel under static and flow conditions using special glass cell for each condition at four temperatures by potentiostat and suggest numerical model to compare the theoretical with experimental results.

EXPERIMENTAL PROCEDURE

Chemical composition of low carbon steel (wt%: 0.077 C, 0.309 Mn, 0.003 Si, 0.0001 P, 0.021 S, 0.0001 Cr, 0.0002 Mo, 0.023 Cu, 0.0001 Ni, 0.003 V and Fe remain) obtained by spectromax in specialized institute for engineering industries. The sample having dimension (17.5x18x3mm) which was used in all experiments

after polishing to mirror finish, degreased with acetone and rinsed with distilled water and then mounted by hot mounting using formaldehyde (Bakelite) at 138°C for 8 minute to insulate all but one side and made a hole on one side to electrical connection. This sample was then dried in open air and stored in desiccators over silica gel for subsequent use.

The base electrolyte was 5% NaCl [27] as brine solution and saturated with CO₂ at 9 and 30ml/min. to study sweet corrosion conditions.

Electrochemical cell was composed of platinum counter electrode, prepared low carbon steel specimen as working electrode and saturated calomel electrode (SCE) as a reference electrode using ASTM standard cell G5-94 [28] for stagnant conditions and certain glass cell for horizontal flow (as occurring in buried pipes) as shown in Figure (1).

The electrochemical behaviour of low carbon steel sample was studied by WINKING M Lab potentiostat by recording anodic and cathodic potentiodynamic polarization curves. Measurements were performed in the 5% NaCl solution in the absence and presence of CO₂ at 9 and 30ml/min. Measurements were carried out by changing the electrode potential automatically at less and more -200 mV around open circuit potential at a scan rate of 3 mV.s⁻¹. The linear Tafel segments of anodic and cathodic curves were extrapolated to corrosion potential to obtain corrosion current densities (i_{corr}).

RESULTS AND DISCUSSION

Electrochemical Behavior

Figures (2) to (4) show the polarization curves of low carbon steel in 5% NaCl solution at four different temperatures in absence and presence of CO₂ at rate of 9 and 30 ml/min. respectively under static conditions.

These curves show the cathodic and anodic regions to estimate the corrosion parameters by extrapolation Tafel method as listed in Table (1). The data of corrosion indicate that the corrosion potential (E_{corr}) shift generally toward noble direction in the presence of CO₂ gas, this means that the potential of the galvanic cell becomes more negative and hence the Gibbs free energy change (ΔG) for the corrosion process becomes more positive respectively. The corrosion reaction is then expected to be less spontaneous on pure thermodynamic ground [29]. It is thus shown that (E_{corr}) value is a measure for the extent of the feasibility of the corrosion reaction on purely thermodynamic basis.

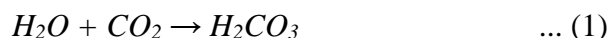
But the thermodynamic prediction don't agreement with kinetics, where it is can be seen that the corrosion current densities (i_{corr}) became higher than that of the case in the absence of CO₂ under static and flow conditions. It is known that any factor

that enhances the value of (i_{corr}) results in an enhanced value of the corrosion rate on pure kinetic ground because of the flowing of medium lead to removal any layers, corrosion products or deposits from the surface and get a more active surface.

Figures (5) to (7) show the polarization curves of low carbon steel in 5% NaCl solution at flow rate of solution 200 L/h, four different temperatures and two different rate of CO₂ respectively. The corrosion parameters of these curves are listed in Table (2).

When compared the flow conditions in the absence and presence of CO₂, can be seen that the E_{corr} shift toward noble direction, while the results of i_{corr} show shifting corrosion current densities toward higher values at 9 ml/min and lower values at 30 ml/min of CO₂. The later result suggests that under flow conditions at 30 ml/min of CO₂, the FeCO₃ scale may be formed which cover the surface and reduce the dissolution of metal.

A precipitated water phase in such a system dissolves CO₂ up to a concentration proportional to the partial pressure of CO₂ in the gas phase. The solubility depends also on the temperature. CO₂ dissolved in water gives carbonic acid [30]:



which is a weak acid, i.e. it dissociates to a minor extent:



At higher pH values (> 6) HCO₃⁻ dissociates further to H⁺ + CO₃²⁻. The pH value is usually lower, so the latter dissociation occurs normally to a very small extent. The cathodic reaction is assumed primarily to follow the equation:



The hydrogen atoms that are adsorbed on the surface are there combined with hydrogen and form hydrogen gas:



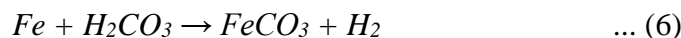
At lower pH values (2–4), reduction of H⁺ from reaction (2) may give a certain contribution, while reduction of HCO₃⁻ is significant at pH > 6.

The cathodic reaction in solutions containing CO₂ may be very efficient and give high current densities. When carbon steel corrodes in water containing CO₂, the

anodic reaction is



The total reaction is



The cathodic reaction in the absence of CO₂ involve reduction of oxygen to hydroxyl ions because of pH of 5%NaCl was equal to 8, while in the presence of CO₂ the cathodic reaction involve reduction of oxygen in addition to reduction reaction that illustrated in eq.(3) and dissociates HCO₃⁻ to H⁺ + CO₃²⁻ [30].

The solubility of FeCO₃ is low and decreases with increasing temperature. FeCO₃ is therefore deposited when the temperature exceeds a limit that depends on the CO₂ partial pressure (often 60–80°C). In the solution, Fe(HCO₃)₂, the formation of which is described by combination of Equations (3) and (4), appears to a considerable extent. At higher temperatures it is decomposed to FeCO₃ and H₂CO₃. When FeCO₃ deposits, protecting film is formed.

Increasing flow velocity causes increasing mass transport and consequently a higher extent of dissolution of corrosion products with increased corrosion rate as a result. The rate (C_R mm/y) of corrosion in a given environment is directly proportional with its corrosion current density (i_{corr}) as follow [31]:

$$C_R = 3.271 \times i_{corr} \times \frac{e}{\rho} \quad \dots (7)$$

Where *i_{corr}* in mA.cm², *e* is equivalent weight of sample in gm, and *ρ* is density of sample in gm.cm⁻³. The data of corrosion rate indicate that the presence of CO₂ with tow flow rates increased the rate compared with the case of absence of CO₂ under static conditions except one case. Under flow conditions, the presence of 9 ml/min. CO₂ increases the corrosion rate, while the presence of 30 ml/min. CO₂ decreases the rate except at 298K as listed in Table (2).

Three Dimensional Results

Figures (8) to (10) show values of three dimensional expermental resultes of corrosion parameters for low carbon steel in 5%NaCl solution, these parameters include corrosion potential (E_{corr}), corrosion current density (i_{corr}), and corrosion rate (C_R) under static conditions at different temperatures in absence and presence of CO₂ at tow rates. While Figures (11) to (13) show values of three dimensional expermental resultes of corrosion parameters for low carbon steel in 5%NaCl solution under flow conditions at different temperatures in absence and presence of CO₂ at two rates.

Mathematical Model

Mathematical modeling is the use of mathematics to describe real-world phenomena, investigate important questions about the observed world, explain real-world phenomena, test ideas and make predictions about the real world. The real world refers to engineering, physics, physiology, ecology, wildlife management, chemistry, economics, sports etc.

We set up a momentum balance of an element at thickness Δr :
 (momentum in) - (momentum out) + force = 0

$$(2\pi r L \tau) |_{r} - (2\pi r L \tau) |_{r+\Delta r} + 2\pi \Delta r \rho g = 0 \quad \dots (8)$$

Divide by $2\pi \Delta r$ and take the limit as $\Delta r \rightarrow 0$

$$\frac{\partial}{\partial r} (r \tau) + r \rho g = 0 \quad \dots (9)$$

Substitution of Newton's Law into this equation gives (for constant μ)

$$\mu \frac{\partial}{\partial r} \left(r \frac{\partial u}{\partial r} \right) = -\rho g r \quad \dots (10)$$

$$\frac{\partial}{\partial r} \left(r \frac{\partial u}{\partial r} \right) = -\frac{\rho g r}{\mu} \quad \dots (11)$$

$$r \frac{\partial u}{\partial r} = -\frac{\rho g}{\mu} \frac{r^2}{2} + C_1 \quad \dots (12)$$

$$\frac{\partial u}{\partial r} = -\frac{\rho g}{\mu} \frac{r}{2} + \frac{C_1}{r} \quad \dots (13)$$

$$\frac{\partial u}{\partial r} = -\frac{\rho g}{2\mu} r + \frac{C_1}{r} \quad \dots (14)$$

By Integration, $\therefore u = \frac{\rho g}{4\mu} r^2 + C_1 \ln r + C_2 \quad \dots (15)$

To find C_1 and C_2 , apply the boundary conditions:

B.C.1 At $r=0$ $u=0$, **B.C.2** At $r=R$

$$\frac{\partial u}{\partial r} = 0$$

From **B.C.1** $C_2=0$, And **B.C.2** $\frac{\partial u}{\partial r} = \frac{\rho g}{4\mu} R + \frac{C_1}{R} = 0$

$$\therefore \frac{C_1}{R} = -\frac{\rho g}{4\mu} R$$

$$\therefore C_1 = -\frac{\rho g}{4\mu} * R^2 \quad \dots (16)$$

$$u = \frac{\rho g}{4\mu} r^2 - \frac{\rho g}{4\mu} R^2 \ln r \quad \dots (17)$$

And the volume rate of flow is: $R_{co2} = \int_0^{2\pi} \int_0^R u r \partial r \partial \theta$. $\dots (18)$

$$R_{co2} = 2\pi \int_0^R u r \partial r \quad \dots (19)$$

$$= \frac{\pi \rho g}{2\mu} \int_0^R (r^2 - R^2 \ln r) r \partial r \quad \dots (20)$$

$$\frac{\pi \rho g}{2\mu} [r^3 - R^2 r \ln r] \quad \dots (21)$$

$$= \frac{\pi \rho g}{2\mu} \left[\frac{r^4}{4} - R^2 \left(\frac{r^2}{2} + \frac{r^2}{2} \ln r \right) \right]_0^R \quad \dots (22)$$

$$= \frac{\pi \rho g}{2\mu} \left[\frac{R^4}{4} - R^2 \left(\frac{R^2}{2} + \frac{R^2}{2} \ln R \right) \right] \quad \dots (23)$$

$$= \frac{\pi \rho g}{2\mu} \left[\frac{R^4}{4} - \frac{R^2}{2} (1 + \ln R) \right] \quad \dots (24)$$

$$\frac{\pi \rho g R^2}{2\mu} \left[\frac{R^2}{4} - \frac{2}{4} (1 + \ln R) \right] \quad \dots (25)$$

$$R_{co2} = \frac{\pi \rho g R^2}{2\mu} \left[\frac{R^2}{4} - \frac{1}{2} (1 + \ln R) \right] \quad \dots (26)$$

Empirical Correlation Corrosion Rate

Dimensional analysis is used to correlate diameter of rate of CO₂, Temp., and E_{corr}, i_{corr}, diameter of pipe, pressure drop and physical properties of gas phase.

$$C_R = f [R_{CO_2}, C_{pCO_2}, E_{corr}, i_{corr}, Tafel\ slope(bc/ba), D_p, \Delta p, \mu_{CO_2}, \rho_{CO_2}, g] \dots (27)$$

Applying Buckingham's II theory for dimensional analysis. The following correlations obtained

$$C_R = \frac{R_{CO_2}^2}{\Delta P^2} B_1 \left\{ \left[\frac{g}{\Delta P^5 R_{CO_2}^2} \right]^{B_2} \left[[\Delta P^2 i_{corr}] \right]^{B_3} \left[E_{corr} \right]^{B_4} \left[\frac{bc}{ba} \right]^{B_5} \left[\frac{DP \Delta P}{R_{CO_2}^2 \rho_{CO_2}} \right]^{B_6} \right. \\ \left. \left[\frac{DP \mu_{CO_2}}{R_{CO_2} \rho_{CO_2}} \right]^{B_7} \left[\frac{DP^4 T C P}{R_{CO_2}} \right]^{B_8} \right\} \dots (28)$$

The constant B₁ and powers at the dimensionless group in Equation (24) were calculated using statistica computer program version 6.5, Table (3) listed the values of constants, correlation coefficient, Variance and standard error.

Finally, Figures (14) and (15) show the comparison between observed, residual and predicated values respectively. This type of figure means that there is agreement between theoretical and experimental results.

CONCLUSIONS

The main conclusions are drawn from the present study are the presence of CO₂ at 9ml/min increase the corrosion rate because of dissolve of CO₂ to form carbonic acid which is dissociates further to H⁺ and carbonate ions and the pH value is usually lower under static and flow condition at rate 200L/h. While the presence of 30ml/min CO₂ increase the corrosion rate only under static conditions and decrease the corrosion rate under flow conditions due to formation of FeCO₃ scale except at 298K. Numerical model shows the agreement of theoretical and experimental results.

REFERENCES

[1]. Waard, C. & Milliams, D. E. (1975). Corrosion, 31, 131.
 [2]. Waard, C., Lotz, U. , Milliams, D. E. (1991) Corrosion, 47, 976.
 [3]. Waard, C., Lotz, U., Dugstad, A. (NACE International, 1995). Influence of Liquid Flow Velocity on CO₂ Corrosion: A Semi-Empirical Model. CORROSION/95, paper no. 128,
 [4]. Bonis, M. R. & Crolet, J.L. (NACE International, 1989) .Basics of the Prediction of the Risks of CO₂ Corrosion in Oil and Gas Wells. CORROSION/89, paper no. 466.

- [5]. Crolet, J.L.& Bonis, M. R. (1991). SPE Production Engineering, 6, 449.
- [6]. Gunaltun, Y.M. (NACE International, 1996).Combining research and field data for corrosion rate prediction. CORROSION/96, paper No. 27.
- [7]. Halvorsen, A. M. K. & Sønvedt, T. (NACE International, 1999). CO₂ Corrosion Model for Carbon Steel Including a Wall Shear Stress Model for Multiphase Flow and Limits for Production Rate to Avoid Mesa Attack. CORROSION/99, paper No.42.
- [8]. Adams, C. D., Garber, J. D., Singh, R. K. (Houston Texas: NACE International, 1996) .Computer Modelling to Predict Corrosion Rates in Gas Condensate Wells Containing CO₂. CORROSION/96, paper no. 31.
- [9]. Srinivasan, S. & Kane, R. D. (Houston Texas: NACE International, 1996) .Prediction of Corrosivity of CO₂ H₂S Production Environments. CORROSION/96, paper no. 11.
- [10]. John, R.C. (Houston Texas: NACE International, 1998) .SweetCor: An Information System for the Analysis of Corrosion of Steels by Water and Carbon Dioxide. CORROSION/98, paper no. 20.
- [11]. Jepson, W. P., Kang, C., Gopal, M., Stitzel, (Houston Texas: NACE International, 1997) .Model for Sweet Corrosion in Horizontal Multiphase Slug Flow. CORROSION/97, paper no. 11.
- [12]. Zhang, R., Gopal, M., Jepson, W. P. (Houston, TX: NACE International, 1997). Development of a Mechanistic Model For Predicting Corrosion Rate in Multiphase Oil/Water/Gas Flows. CORROSION/97, paper no. 601.
- [13]. Pots, B. F. M. (Houston Texas: NACE International, 1995) .Mechanistic Models for the Prediction of CO₂ Corrosion Rates under Multi-Phase Flow Conditions. CORROSION/95, paper no. 137.
- [14]. Anderko, A. & Young, R. (Houston, TX: NACE International, 1999).Simulation of CO₂/H₂S Corrosion Using Thermodynamic and Electrochemical Models. CORROSION/99, paper no. 31.
- [15]. Dayalan, E., Moraes, F. D., Shadley, J. R., Shirazi, S. A., Ribicki, E. F. (Houston, TX: NACE International, 1998).CO₂ Corrosion Prediction in Pipe Flow Under FeCO₃ Scale-Forming Conditions. CORROSION/98, paper no. 51.
- [16]. Sundaram, M. , Raman, V., High, M. S., Tree, D. A., Wagner, J. (Houston, TX: NACE International, 1996).Deterministic Modeling of Corrosion in Downhole Environments. CORROSION/96, paper no. 30.
- [17]. High, M. S., Wagner, J., Natarajan, S. (Houston, TX: NACE International, 2000).Mechanistic Modelling of Mass Transfer in the Laminar Sublayer in Downhole Systems. CORROSION/2000, paper no. 62,
- [18]. Ethirajulu, D., Moraes, F.D., John R., Edmund F., and Siamack A.(1998). CO₂

- Corrosion Prediction in Pipe Flow Under FeCO₃ Scale-Forming Conditions. CORROSION /98, March 22 - 27.
- [19]. Anthony K & Srdjan N. (1999). Prediction of two-phase erosion – corrosion in bends. Second International Conference on CFD in the Minerals and Process Industries CSIRO, Melbourne, Australia, 6-8 December.
- [20]. Killian D. (2000). Jet Impingement Testing for Flow Accelerated Corrosion. CORROSION 2000, March 26 - 31.
- [21]. Energy Resour. Technol. (June 2001) .Mass Transfer Coefficient Measurement in Water/Oil/Gas Multiphase Flow.,CORROSION, 123(2), 144-150.
- [22]. Rolf N.,(2003).Corrosion control in oil and gas pipelines. Technology over view pipeline, 3, 2-3.
- [23]. Srgjan Nestic, Shihuai Wang, Jiyong Cai and Ying Xiao,(2004).Integrated CO₂ corrosion-multiphase flow model. Institute for Corrosion and Multiphase Technology, 4626.
- [24]. Shunsuke Uchida, Masanori Naitoh, Hidetoshi Okada, Yasushi Uehara, Seiichi Koshizuka, Robert Svoboda, and Derek H. Lister,(2009) .Effects of Water Chemistry on Flow Accelerated Corrosion and Liquid Droplet Impingement Accelerated Corrosion. Power Plant Chemistry ,11(12).
- [25]. Mohammed Nor A., Suhor M.F., Mohamed M.F., Singer M. and Nestic S.,(2011). “Corrosion of carbon steel in high CO₂ environment flow effect”. Published by Nace International, No. 11242.
- [26]. Asmara Y.P., Ismail M.C.,(2011).Study combinations effects of acetic acid in H₂S/CO₂ corrosion. Journal of applied science, 11(10), 1821-1826.
- [27]. Jackman P.S. and Smith, L.M. (1999).Advances in corrosion control and materials in oil and gas production. Published for the European Federation of Corrosion by IOM Communications, 386.
- [28]. ASTM G5-94 (Reapproved 2004), “Standard Reference Method for Making Potentiostatic and Potentiodynamic Anodic Polarization Measurements”.
- [29]. Rana A. Majed, “Thermodynamic and kinetic study for the corrosion of aluminium”, Lambert Academic Publishing, 2013.
- [30]. Einar Bardal, “Corrosion and Protection”, Springer, Chapter 6, p.78, 2003.
- [31]. Pierre R. Roberge, “Handbook of Corrosion Engineering”, Mc Graw –Hill, 2000.

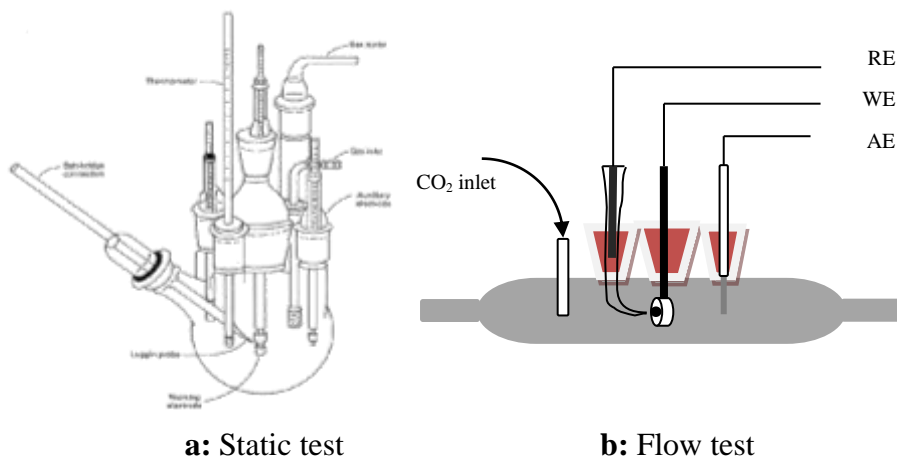


Figure (1) Glass cell for electrochemical measurements.

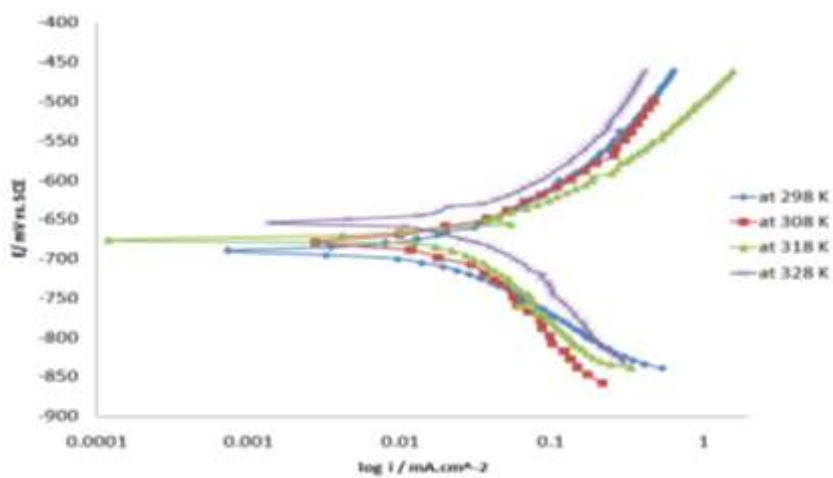


Figure (2) Potentiodynamic curve for low carbon steel in 5% NaCl solution under static conditions at four Temperatures in the absence of CO₂.

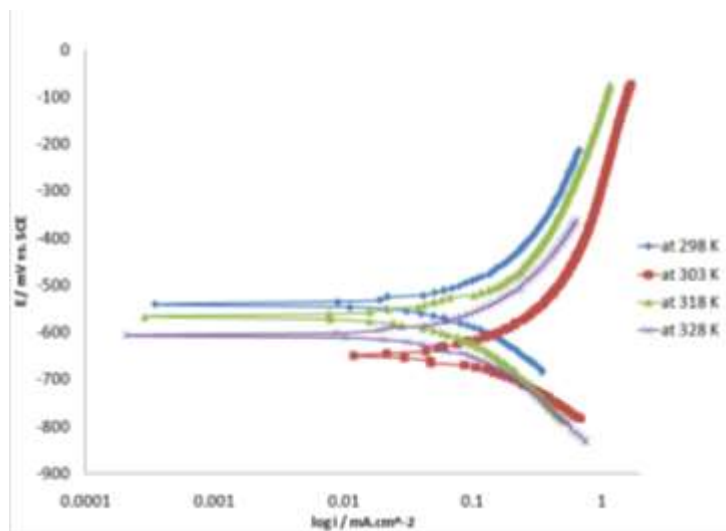


Figure (3) Potentiodynamic curve for low carbon steel in 5% NaCl solution under static conditions at four temperatures in the presence of CO₂ at rate 9ml/min.

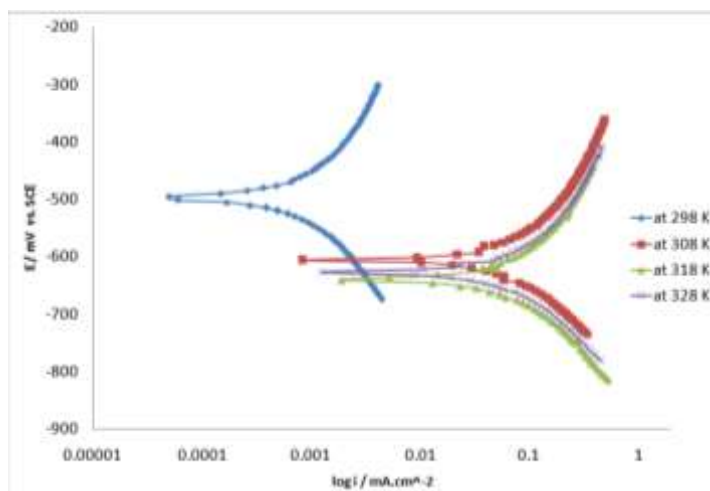


Figure (4) Potentiodynamic curve for low carbon steel in 5% NaCl solution under static conditions at four temperatures in the Presence of CO₂ at rate 30ml/min.

Table (1) Corrosion parameters of low carbon steel in 5%NaCl solution include corrosion potential (E_{corr}), corrosion current density (i_{corr}), cathodic and anodic Tafel slopes (bc & ba), and corrosion rate (CR) under static conditions at different temperatures in absence and presence of CO₂ at tow rates.

Rate of CO ₂	Temp. K	E _{corr} mV	i _{corr} µA/cm ²	Tafel slope (mV.dec ⁻¹)		CRx10 ⁻³ mm/y
				-bc	+ba	
0 ml/min.	298	-679.0	14.23	92.8	95.9	166.58
	308	-659.4	28.51	169.0	99.9	333.76
	318	-681.4	24.57	128.9	80.9	287.63
	328	-721.0	32.42	127.8	97.7	379.537
9ml/min.	298	-538.8	33.91	106.9	103.2	396.981
	308	-650.8	38.71	62.7	76.8	453.174
	318	-569.8	25.72	97.3	88.1	301.101
	328	-605.8	33.45	106.2	99.1	341.256
30ml/min.	298	-497.0	58.67	20.2	23.8	686.844
	308	-607.0	29.27	97.5	98.9	342.661
	318	-640.4	28.53	100.1	97.3	33.998
	328	-644.4	23.85	72.7	91.1	305.5

Table (2) Corrosion parameters of low carbon steel in 5%NaCl solution include corrosion potential (E_{corr}), corrosion current density (i_{corr}), cathodic and anodic Tafel slopes (bc & ba), and corrosion rate (C_R) under flow conditions at 200L/h and different temperatures in absence and presence of CO₂ at tow rates.

Rate of CO ₂	Temp. K	E _{corr} mV	i _{corr} µA/cm ²	Tafel slope (mV.dec ⁻¹)		CRx10 ⁻³ mm/y
				-bc	+ba	
0 ml/min.	298	-689.7	18.31	112.5	108.5	214.353
	308	-679.7	28.54	218.8	126.2	334.115
	318	-676.5	22.15	139.2	81.8	259.308
	328	-674.9	24.46	160.7	80.2	286.35
9ml/min.	298	-649.0	28.78	172.4	101.3	336.924
	308	-670.4	29.60	182.7	82.4	346.524
	318	-673.6	25.55	122.9	52.5	299.111
	328	-733.0	31.11	202.4	93.5	275.931
30ml/min.	298	-610.9	42.29	34.7	18.1	495.085
	308	-673.5	7.66	104.4	97.1	89.674
	318	-674.3	6.33	88.5	108.2	74.104
	328	-700.0	6.25	123.8	133.9	73.168

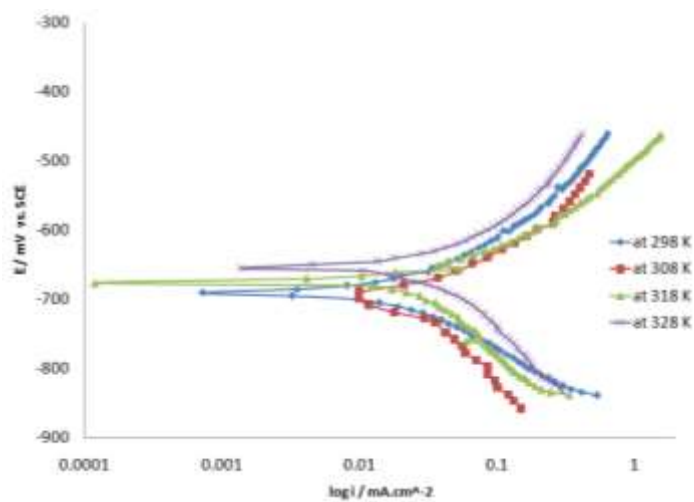


Figure (5) Potentiodynamic curve for low carbon steel in 5% NaCl Solution under flow conditions at 200 L/h and four Temperatures in the absence of CO₂.

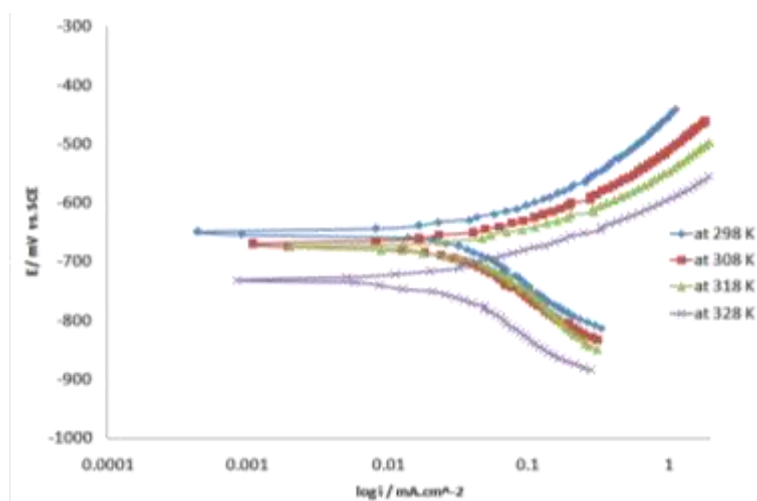


Figure (6) Potentiodynamic curve for low carbon steel in 5% NaCl Solution under flow conditions at 200 L/h and four Temperatures in the presence of CO₂ at 9ml/min.

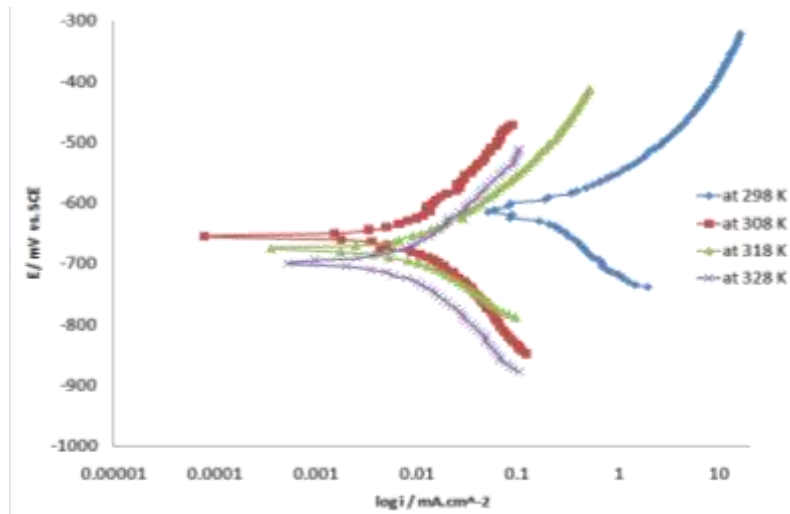


Figure (7) Potentiodynamic curve for low carbon steel in 5% NaCl Solution under flow conditions at 200 L/h and four temperatures in the presence of CO₂ at 30ml/min.

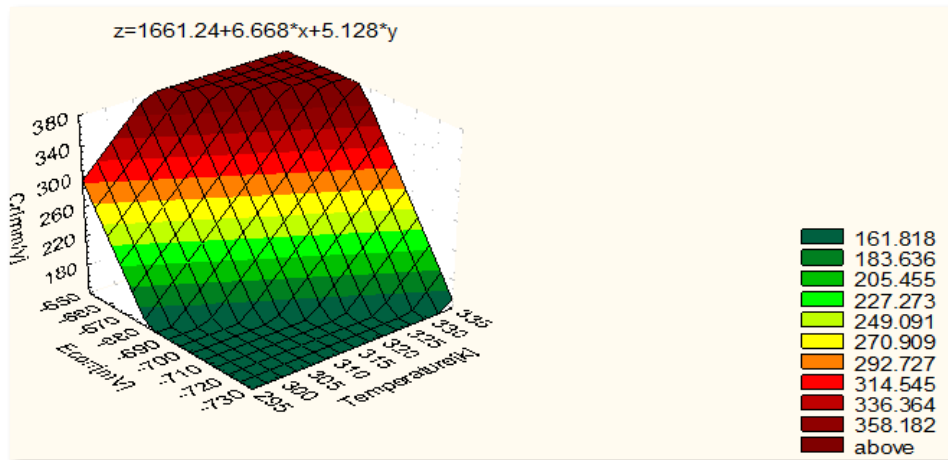


Figure (8) Effect of Temp and E_{corr} on C_R under static condition in the absence of CO₂.

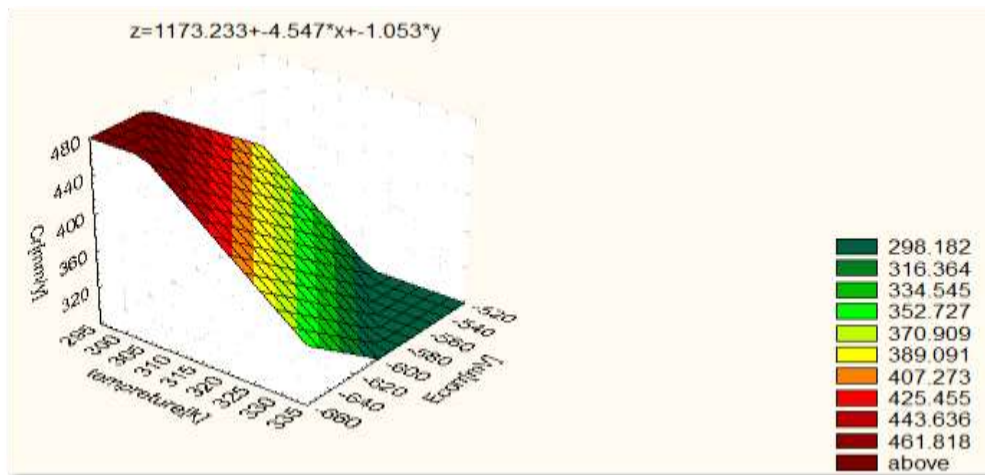


Figure (9) Effect of Temp and E_{corr} on C_R under static Condition in the presence of 9ml/min CO₂.

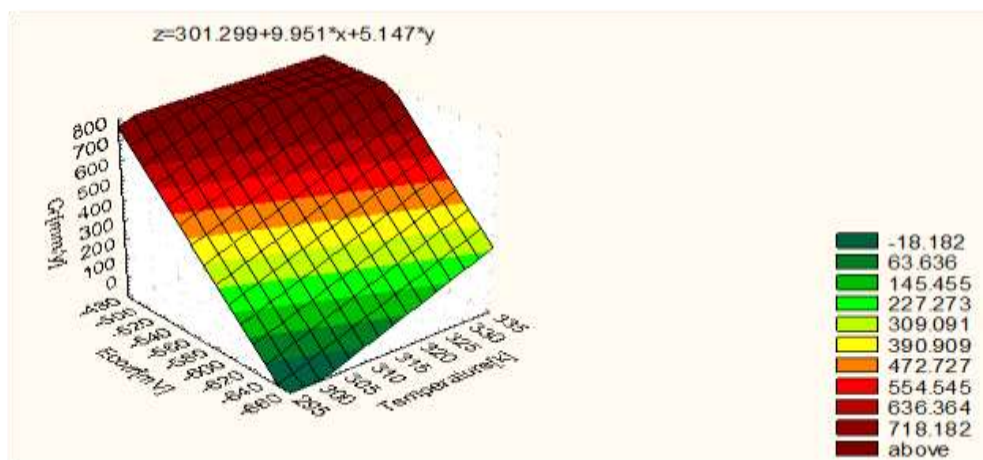


Figure (10) Effect of Temp. and E_{corr} on C_R under static condition in the presence of 30ml/min CO₂.

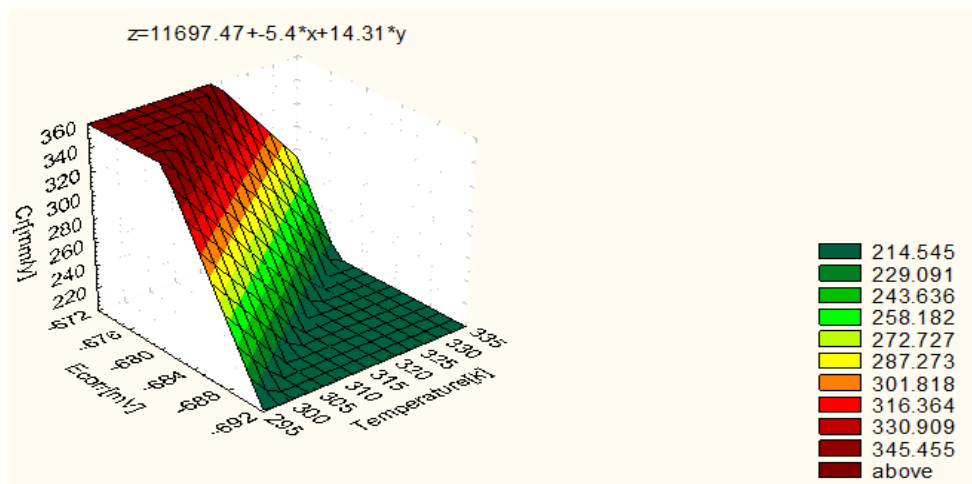


Figure (11) Effect of Temp. and E_{corr} on C_R under flow condition in the absence of CO₂.

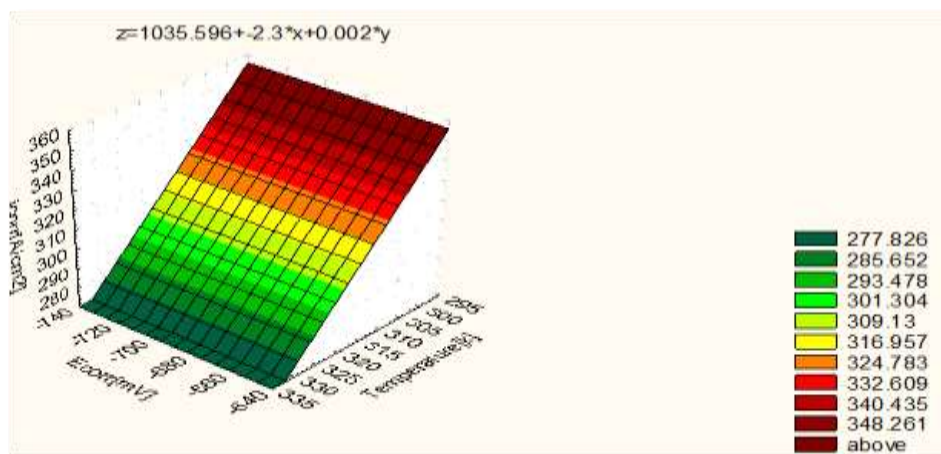


Figure (12) Effect of Temp. and E_{corr} on C_R under flow condition in the presence of 9ml/min CO₂.

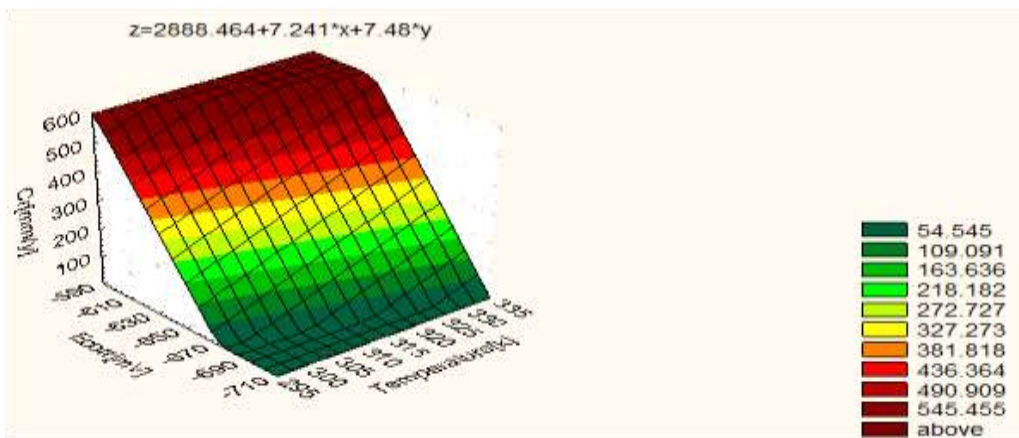


Figure (13) Effect of Temp. and E_{corr} on C_R under flow condition in the presence of 30ml/min CO₂.

Table(3)_ Value of parameters for equation 24.

B ₁	B ₂	B ₃	B ₄	B ₅	B ₆	B ₇	B ₈	R	Variance explained
0.607431	-1.04347	4.343141	-4.61105	0.516501	1.618761	-0.61905	-3.40973	1.00000	10000

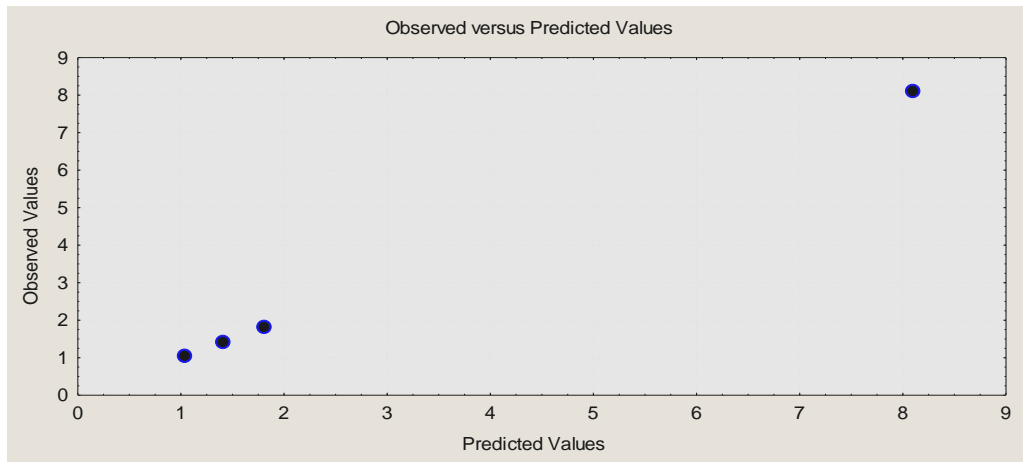


Figure (14) Comparison between the observed and predicted results of C_R (mm/y).

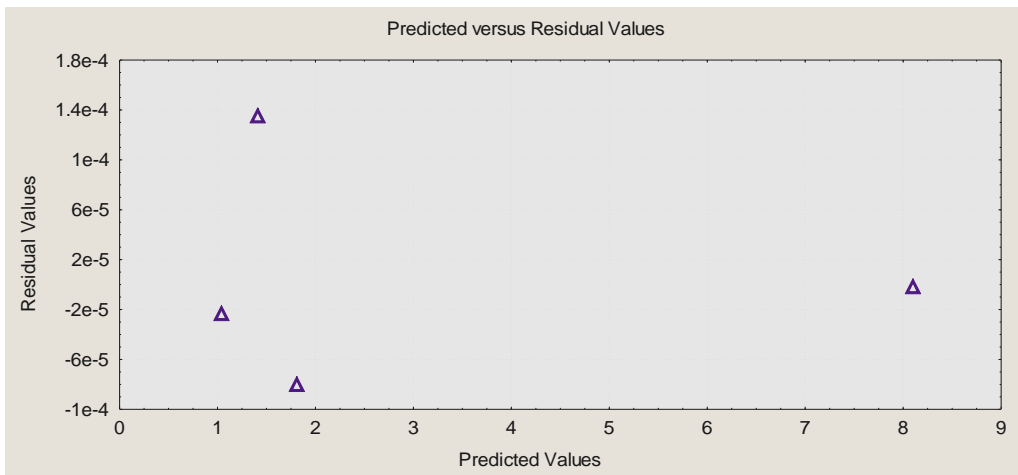


Figure (15) Comparison between the residual and predicted results of C_R (mm/y).